

INTERFACE MODEL TO FIRE-THERMOMECHANICAL PERFORMANCE-BASED ANALYSIS OF STRUCTURES UNDER FIRE CONDITIONS

Julio Cesar G. Silva, Alexandre Landesmann and Fernando L.B. Ribeiro

Civil Engineering Program, Federal University of Rio de Janeiro (COPPE/UFRJ)
Laboratory of Structures and Materials - Numerical Modeling
Rio de Janeiro/RJ, POB 68.506, 21945-970, Brazil
e-mail: jcsilva@coc.ufrj.br

ABSTRACT

This work is dedicated to the development of a computational model to perform an interface for fire-thermomechanical performance-based analysis of structures under fire conditions. The proposed analysis procedure links the fire-driven fluid flow model, developed with the code Fire Dynamics Simulator (FDS), and a structural thermomechanical analysis via ANSYS commercial package, including large displacements and material plasticity. The developed interface is capable of processing the results from the fire simulation for accounting properly the heat transfer by convection and radiation between the fire and the exposed surfaces (based on Adiabatic Surface Temperature concept) performing the coupling between those two fields.

In this paper, the proposed methodology is applied to a simple case in order to verify the interface against FDS results. This case demonstrates that the interface can account properly the heat transfer from fires to exposed surfaces. Then, the methodology is used to evaluate the fire-thermomechanical behavior of an H-profile column under a localized fire. At the end of analysis it is possible to obtain the structural behavior under specific fire scenarios. In these applications, both solid and shell elements are used demonstrating that the procedure can be applied to evaluate the global behavior of structures. The achieved results also indicate that the suggested methodology can provide reliable performance-based analyses.

INTRODUCTION

Traditionally, the behavior of structures under fire conditions have been achieved by prescriptive simplified procedures, widely available at international codes and standards, e.g., AISC-LRFD (2005), EN 1991-1-2 (2002), EN 1993-1-2 (2005), etc., generally focused on checking if structure members meet the required fire resistance time.

Nowadays, advanced numerical models based on Finite Element Method (FEM) can predict the global behavior of structures including large displacements and material nonlinearities. However, the application

of these models to fire conditions is generally based on simplified temperature-time curves (EN 1991-1-2, 2002). Those functions cannot represent accurately the fire development and it does not account the three-dimensional fuel distribution or the fire compartment geometry.

On the other hand, numerical models based on the Computational Fluid Dynamics (CFD) are capable to provide a reliable description of fire evolution, making it more accessible to simulate the actual fire dynamics for different scenarios. Even with all the efforts related to develop each side separately, a coupled fire-thermomechanical analysis (CFD-FEM) is a relatively new area of research. This coupling is not trivial, the intrinsic differences between those two models, e.g., algorithms, time scales, mesh sizes, etc., make this an encouraging task.

After the collapse of the World Trade Center towers, Prasad and Baum (2005), proposed an interface between the Fire Dynamics Simulator (FDS, McGrattan *et al.*, 2010) and the ANSYS package (SAS, 2009) to investigate the behavior of structural elements during this event. This method was called Fire Structural Interface (FSI) and assumed that the heat transfer between fire and exposed surfaces was given only by radiation. A few time later, a european research project called FIRESTRUC (Kumar *et al.*, 2006) analyzed a number of ways to perform an interaction between CFD and FEM codes focusing in the behavior of structures under fire. Among the CFD codes, FDS has the advantage of include a combustion model to address the fire growth. One of the big concerns stated at this report was related to determine which variables should be transferred from fire simulation to FEM models.

The Adiabatic Surface Temperature (AST) was proposed by Wickström *et al.* (2007) as a variable capable of describing complex convective and radiative conditions into one single scalar quantity. Following this work, an interface between FDS and ANSYS was presented by Duthinh *et al.* (2008), using the AST concept. In that work, a coupling procedure was applied to structural members such as trussed beams.

The main purpose of this paper is to provide a Fire-Thermomechanical Interface (FTMI) model to performance-based analysis of structures under fire conditions. This automated code improves the reach of the fire engineering allowing the simulation of the behavior of global structures, discretized with shell and/or solid elements, under fire conditions. In the next chapters the methodology to describe the FTMI is presented. At this moment, FDS is employed for the fire simulation and ANSYS is used for the thermomechanical analysis, but FTMI methodology can be applied to other CFD and FEM codes. Application examples are provided to verify FTMI and its use for solids and shell elements. Conclusions are presented at the end of the paper.

METHODOLOGY

The description of structural behavior under fire conditions by a fire-thermomechanical model is related to a domain that includes the structure itself and its components, where the thermal energy and the mechanical loads are distributed, combined with the surroundings of the structure, to capture flames and hot gases dynamics. Unfortunately, this coupled fluid-solid problem needs distinct techniques to address the physical phenomena involved, and the solution by a unique domain crashes on the differences between these techniques, as cells or elements dimensions and shapes, algorithms and time steps.

The procedure described in this paper decomposes this domain, described above and illustrated in Figure 1, into two parts: the first one is devoted to fire simulation and the second is about the thermomechanical behavior. At the fire simulation, the structures geometry is simplified and the domain is amplified to capture properly the fire propagation and the smoke and hot gases flow, as shown in Figure 1b. At the thermomechanical analysis, just the structure is modeled and the fire simulation is represented by heat fluxes, applied as boundary

conditions at the exposed surfaces, as exposed in Figure 1c, this approach is commonly referred as one-way coupling. In order to exchange data, both models have the same coordinate system and a consistent geometry (Figure 1).

Heat can be transferred from flames and hot gases to structures surfaces by radiation and convection. So, the total heat flux (q_{tot}^*) can be defined by the sum of these two parcels:

$$q_{tot}^* = \varepsilon \left[e_{r,inc}^* - \sigma(T_s + 273)^4 \right] + h(T_g - T_s) \quad (1)$$

where ε is emissivity, $e_{r,inc}^*$ [W/m^2] is the incident radiative thermal energy, σ [$\text{W}/(\text{m}^2 \cdot \text{K}^4)$] is the Stefan-Boltzmann constant, T_s [$^{\circ}\text{C}$] is the surface temperature, h [$\text{W}/(\text{m}^2 \cdot ^{\circ}\text{C})$] is the heat transfer coefficient and T_g [$^{\circ}\text{C}$] is the gas temperature.

Advanced fire simulation models, as the code used in this paper, are efficient to provide results that characterize the three-dimensional evolution of the fire, incident radiative thermal energy on the exposed surfaces and gas temperatures. However, those are not capable of evaluate precisely temperature distribution on solids. Consequently, the total heat flux, as presented on Eq. (1), cannot be accurately calculated at the end of the fire simulation. Then, an additional approach is necessary to transpose this barrier, adding a supplementary treatment to the exposed surfaces.

Surface thermal exposure

In order to establish an accurate interface between the fire simulation and the thermomechanical analysis, the Adiabatic Surface Temperature concept is used (Wickström, 2004). Considering that the real surface can be replaced by a perfect insulator exposed to the same heating conditions, the total heat flux to this ideal surface is by definition zero (Wickström *et al.*, 2007):

$$\varepsilon \left[e_{r,inc}^* - \sigma(T_{AST} + 273)^4 \right] + h(T_g - T_{AST}) = 0 \quad (2)$$

The fire-structural domain is decomposed into two parts

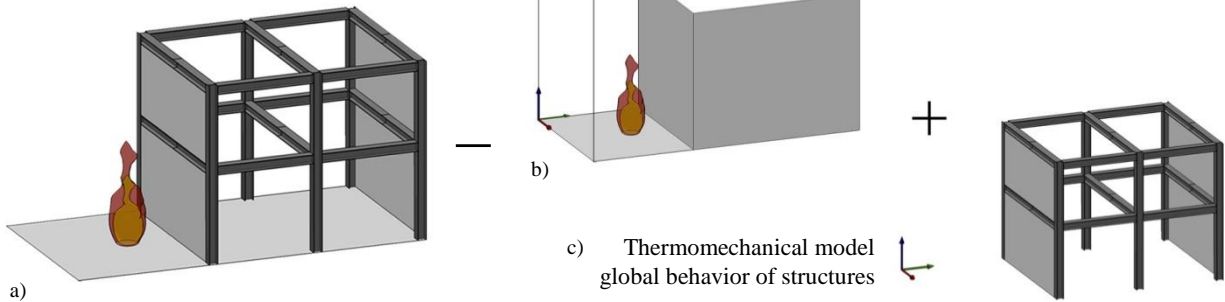


Figure 1: Illustration of the coupled field domain decomposition: a) problem description; b) fire simulation domain; c) thermomechanical model discretization.

and the temperature of this idealized surface, referred here as Adiabatic Surface Temperature (T_{AST}) can be obtained as an output from the fire simulation (McGrattan *et al.*, 2013).

Since the real and the hypothetical surfaces are exposed to the same heating conditions, the total heat flux that will be applied at the thermomechanical model can be obtained by the solution of the system formed by Eqs. (1) and (2):

$$q_{tot}'' = \varepsilon\sigma \left[(T_{AST} + 273)^4 - (T_s + 273)^4 \right] + h(T_{AST} - T_s) \quad (3)$$

This concept transposes the total heat flux dependence on surface temperature at fire simulation (Wickström *et al.*, 2007). It is considered capable of combine the complexity of the fire simulation into one simple scalar by several previous researches, among them: (Wickström *et al.*, 2007; Duthinh *et al.*, 2008; Sandström *et al.*, 2009; Wickström *et al.*, 2010).

Nevertheless, the present methodology considers that to achieve a correct definition to the total heat flux, accounting correctly both the convective and radiative heat fluxes, is also necessary to add the convective heat transfer coefficient (h). Following normative procedures (EN 1991-1-2, 2002) this variable is usually considered as a constant value (Duthinh *et al.*, 2008), but its value can express how important is the convective heat flux for the specific scenario (relative to the radiative heat flux), and also, its spatial distribution and evolution during the fire elapsed time can help to precisely reproduce the heat flux calculated in fire simulation to the thermomechanical analysis.

These two variables (T_{AST} , h) will be denominated here as surface “thermal exposure”. After the fire simulation, the heat flux is evaluated at the thermomechanical model using the Eq. (3), depending on the surface thermal exposure (T_{AST} , h) obtained by the fire simulation, and the surface temperature (T_s), calculated at each time step during the thermomechanical analysis.

Models which geometries do not match perfectly

Part of the intrinsic differences between these two models is related to discretization approach, i.e., the size and shape of the cells or elements used in each field. While in the fire simulation the domain is divided into rectangular cells (or hexahedrons) in a rectilinear grid, for the thermomechanical analysis the structure is usually discretized with solids or shells elements. Also, the element size needed to achieve a correct solution at the thermomechanical model can lead to an unfeasible fire simulation. Therefore, even for the most modest structures, with the simplest geometries, the models generated for each side of this interface do not match perfectly.

In order to establish the connection between these two fields, the external faces of the elements (FEM), which correspond to the exposed surfaces, need to be mapped against the available fire simulation results. Moreover, some of these variables, as T_{AST} and h , are dependent of orientation of the cell face where they are calculated and this orientation needs to be accounted before the results been prescribed as boundary conditions. This mapping is realized by a collection of **I** keypoints (of **x** coordinates) localized at the center of each external face (with normal **n**), as illustrated in Figure 2. The position and the number of **I** keypoints is based on the mesh generated for the thermomechanical analysis. In this way, the coupling procedure can be achieved for different discretization levels. Also, small modifications and dimensioning does not imply in restarting all the process, as the structures geometry is simplified on the fire simulation.

With the intention of map the different models and get these results automatically, a code called `fds2ftmi` was created. This code is based on `fds2ascii` routine, available on the FDS package (McGrattan *et al.*, 2013). Basically, `fds2ftmi` traces down the exposed surfaces at ANSYS, defines and collects the **I** keypoints and the corresponding **n** directions (related

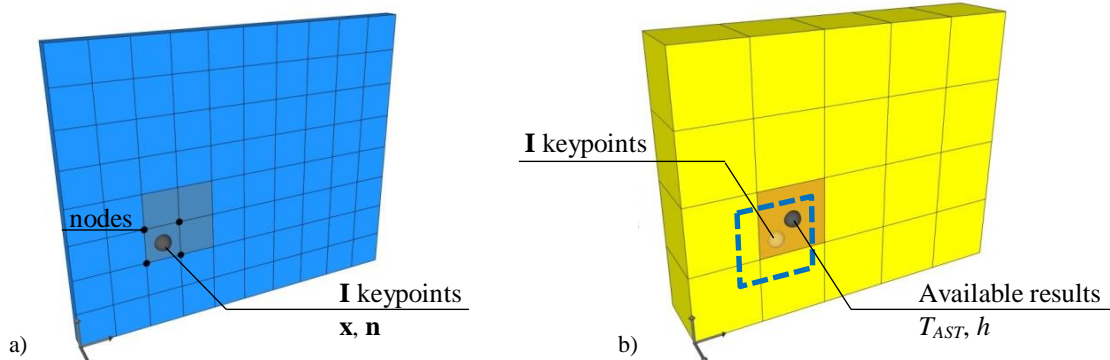


Figure 2: Illustration of the exposed surfaces and the mapping procedure: a) thermomechanical model; b) fire simulation.

to the element surface). Then, based on each **I** keypoint position the code is able to search into the boundary results file (.bf) from FDS, iterates over time, orientations and meshes, to transcript the correct surface thermal exposure results (T_{AST} , h) into a ANSYS APDL language script file.

The described procedure can be easily understood for solid elements with aligned surfaces (Figure 2). Nevertheless, the extension of this procedure to more kinds of elements and geometries is a more challenging task. For geometries discretized with shell elements, `fds2ftmi` places **I** keypoints at both sides of this plane element to capture the correct orientation, by normal direction, and thermal gradient through shell layers. A further discussion about the application of this procedure for complex geometries, curved or oblique to the Cartesian axis, will be handled together with the presented results.

Heat flux into FEM models

At the FEM model, the main target related to this interface procedure is create an iterative solution capable to use the surface temperature, obtained at each time step, to evaluate the heat flux at each node of the exposed surface through Eq. (3). Therefore, the surface effect element SURF152 (ANSYS nomenclature) is employed; this element can apply a heat flux vector (\mathbf{q}_{nodes}) at each node of the exposed surface based on: surface area (A_{elem}), normal vector (\mathbf{n}) and number of surface nodes (n_{nodes}), as illustrated in Figure 3. In this task, the T_{AST} is prescribed at the elements extra node and h is applied at the elements surface (Figure 3). If this procedure is used with shell elements, the heat flux vector is calculated and prescribed at the top and bottom layers of the shell section.

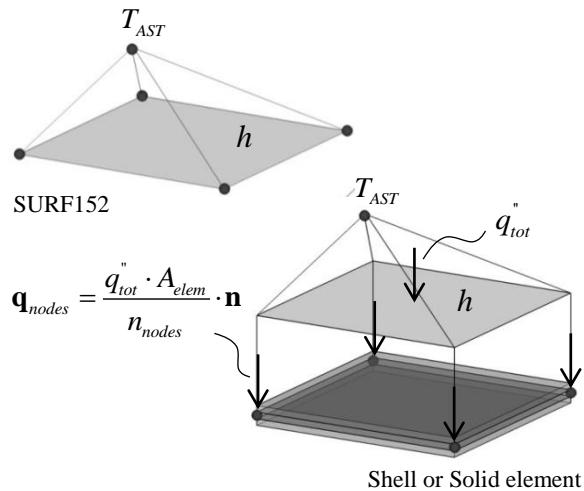


Figure 3: Illustration of the thermal exposure (T_{AST} , h) transcription into boundary conditions by SURF152 element.

APPLICATION

This chapter presents the application examples proposed and a discussion about the results. In the first case, a simple panel is used to verify the FTMI against FDS results. This case verifies that the interface can translate correctly the heat flux from fire simulations to thermomechanical models. Then, the methodology is used to demonstrate the use of FTMI to evaluate the mechanical behavior of an H-profile column under a localized fire.

FTMI verification case

In order to verify FTMI, a steel panel is exposed to a localized fire and the temperature distribution obtained is compared with FDS results. Since FDS has a 1D thermal conduction model; a plane steel panel is used in this case. The structure is also aligned with the Cartesian coordinates (parallel to yz plane), with 1.5m width, 1.0m height and 1cm thick, as illustrated in Figure 4. The distance between the plane and the fire source is 30cm. The simulation domain is a 1.5x1.5x2m open box and the fire scenario is the leakage of 0.1liters/min of methane at 2m/s. The main goal is to analyze if FTMI is capable of create an interface that reproduces the heat transfer between flames and hot gases (from CFD) to structures surfaces (FEM).

The surface temperature obtained by both methods (FDS and FTMI) will be compared. The FDS thermal model will not be able to capture the heat conduction across the panel (in yz plane - Figure 4), which is important if the material has a high thermal conductivity, as the case of steel. Then, to match both thermal models and keep the comparison at the level of the interface between the gas and solid phases, the ANSYS model is configured to perform just 1D conduction through the panel (x axis).

The adiabatic surface temperature (T_{AST}) distribution at 5min of fire elapsed time is presented at Figure 4a. The central region of the panel has the highest results and the distribution is close to a radial function, but the flame shape changes the circular pattern to a more elliptical silhouette. The evolution of the thermal exposure is presented in Figure 5. As expected, the T_{AST} is almost steady and it will reduce as the surface temperature increases (around 400°C at A and D and 150°C at C and F - Figure 5b). The heat transfer coefficient is dependent of the velocity field close to the surface, generating oscillations at the higher points of the plane (A, B and C - Figure 5b).

After the fire simulation, the thermal exposure results are prescribed as boundary conditions at the thermal model using FTMI (and `fds2ftmi`). The surface temperature(T_s) distribution for this 1D thermal

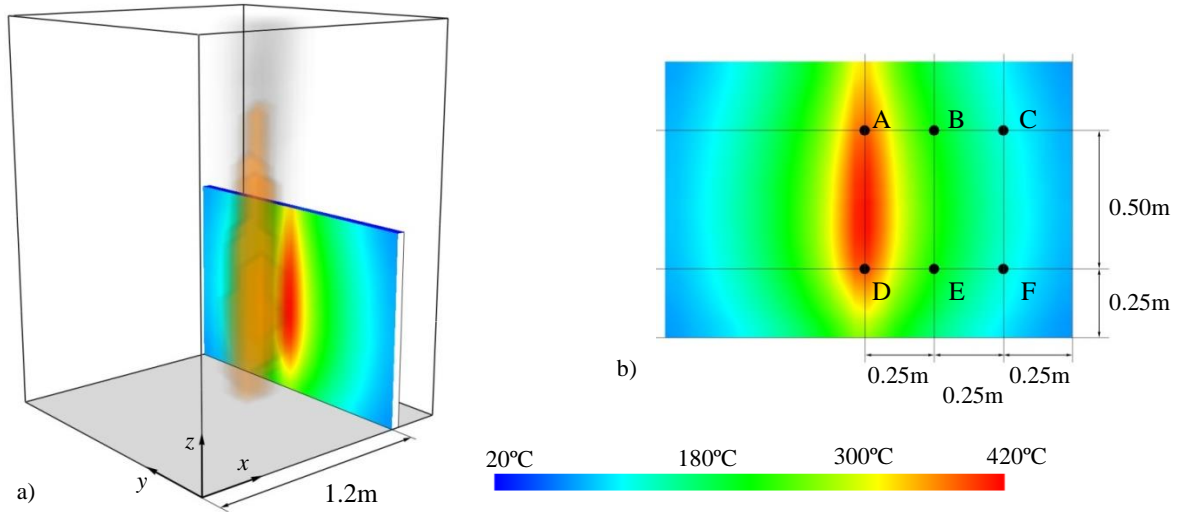


Figure 4: Illustration of the fire scenario with T_{AST} distribution at 5 min: a) 3D model; b) frontal view.

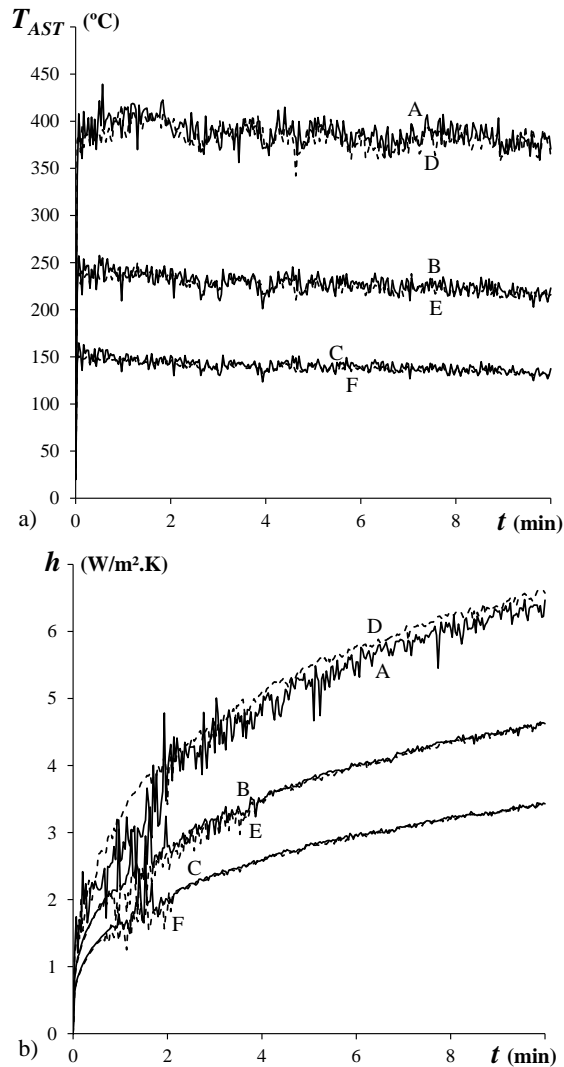


Figure 5: Evolution of the thermal exposure: a) adiabatic surface temperature (T_{AST}); b) heat transfer coefficient (h).

model is illustrated in Figure 6. The T_s distribution has the same profile than T_{AST} (Figure 4), but with higher concentration in central region. The addition of h distribution in FTMI (which also has higher values at central region - Figure 5b) amplifies the heat flux (Eq. 3), increasing the temperature gradient at this region. At 10min of simulation, T_s at A is 164.4°C and just 68.7°C at C, which correspond to 42% of T_s at A; at the same instant, the T_{AST} at C is 60% of the T_{AST} at A.

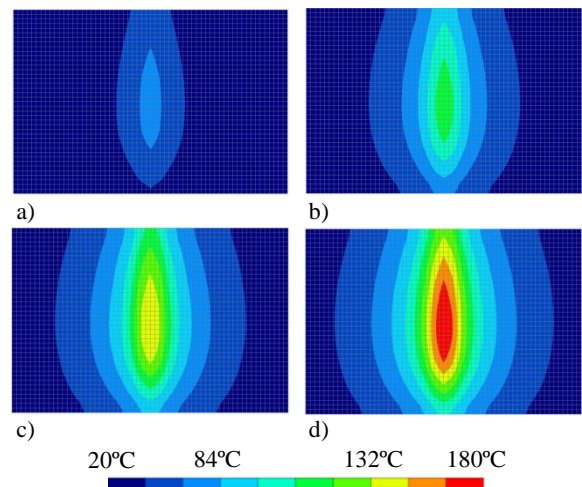


Figure 6: Distribution of the surface temperature: a) 2min; b) 5min; c) 7.5min; d) 10min (1D thermal model).

The comparison between the surface temperature evolution obtained by FTMI and FDS is presented in Figure 7. According to these results, the methodology is capable of replicate in FEM the boundary conditions involved in this phenomenon. The maximum difference between the results is about 0.5% (at A) which is considered a great correlation.

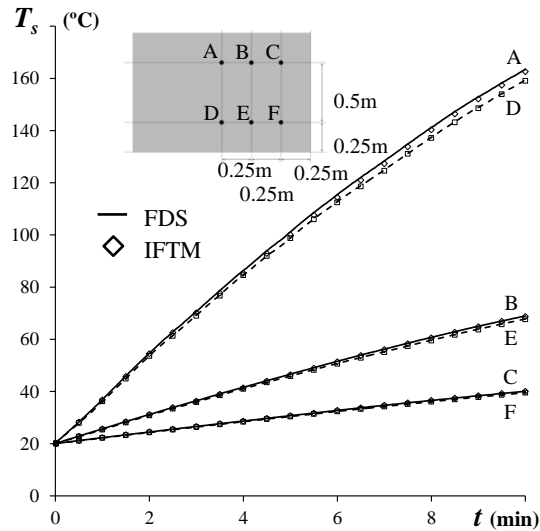


Figure 7: Evolution of surface temperature, comparison between FTMI (1D) and FDS results.

Based on this correlation is possible conclude that FTMI accomplished the task of compute correctly the heat transfer between solid and gas phases. Is important to keep in mind that ANSYS thermal model was modified to match FDS 1D heat conduction model into this verification case. FTMI (FEM thermal model) is capable of 3D heat conduction, which will provide a better temperature distribution even for simple cases like this one.

H-profile column

In this case a simple supported H-profile column is exposed to a localized fire. The steel column is 3m height and the cross section is 0.3m (flange) x 0.4m (web), with a 12.5mm thickness web and 16mm thickness flanges. The fire scenario is a 200kW pool fire (20x20cm) located 40cm (from pool center) to the web, as illustrated in Figure 8. The steel properties are considered temperature dependent as suggested in EN 1993-1-2 (2005).

The column is discretized with shell elements (FEM) to demonstrate the applicability of FTMI to shell structures. Each side of these plane elements will have a different thermal exposure (shadow effect), incident radiation and gas temperature around the surface. So, the proposed methodology is designed to address this singularity and prescribe the correspondent heat flux at the shell elements top and bottom layers.

The T_{AST} distribution at 15min of fire elapsed time is presented on Figure 8. The pool fire is close to the column, so the part facing the fire will be hotter than the other parts of the cross section, being possible to observe the shadow effect at the flanges close to the

fire source (Figure 8a). The FEM model is presented on Figure 8b where some points are highlighted to link with the results.

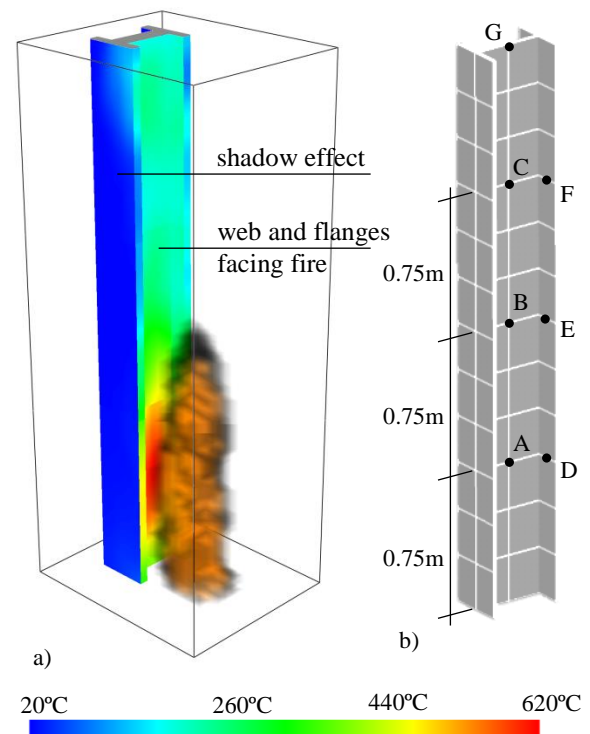


Figure 8: Illustration of the H-profile column localized fire scenario with T_{AST} distribution at 15 min: a) 3D model; b) FEM model.

The adiabatic surface temperature results for each side of the flange elements can be compared to illustrate the improvement related to include the shadow effect in this model. The T_{AST} evolution for points: D, E and F, located at a flange close to the fire source (Figure 8b), are presented on Figure 9 (the subscript 1 is related to the layer facing the fire source and subscript 2 means the layer facing outwards). At D_1 , the T_{AST} is about 550°C during the fire developed phase, and for D_2 the average result is 35°C. Since D_2 is not facing the fire, this result comes from the hot gases that flow around this point. The heat flux needs to be accounted at the points not facing the fire to include the cooling provide by heat exchange at those points, which can increase the temperature gradient inside the flange. At E and F this effect is also present, at E_1 and F_1 the T_{AST} are around 325°C and 175°C, for E_2 and F_2 they are 32°C and around 20°C, respectively.

According to the prescriptive values presented at EN 1991 (2002), a heat transfer coefficient of 25W/(m².°C) should be used for ISO834 curve, this value was also used by Duthinh *et al.*, (2008). At this

case, the maximum h for the points at the flange is achieved at F_1 , which average is $11.4\text{W}/(\text{m}^2\cdot^\circ\text{C})$. At D_1 and E_1 , it is $9.6\text{W}/(\text{m}^2\cdot^\circ\text{C})$ and $9.25\text{W}/(\text{m}^2\cdot^\circ\text{C})$ respectively. At F_2 this variable is $5.23\text{W}/(\text{m}^2\cdot^\circ\text{C})$, which is more close to the $4\text{W}/(\text{m}^2\cdot^\circ\text{C})$ presented at EN 1991-1-2 (2002) for unexposed surfaces. Even tough, for the also unexposed points D_2 and E_2 , these results are $7.09\text{W}/(\text{m}^2\cdot^\circ\text{C})$ and $5.9\text{W}/(\text{m}^2\cdot^\circ\text{C})$. These differences can illustrate that this variable should not be considered as a constant value.

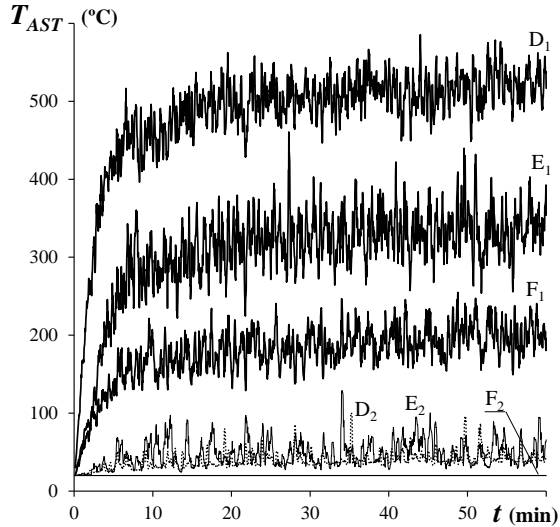


Figure 9: Evolution of the adiabatic surface temperature (T_{AST}) in function of fire elapsed time.

The distribution of the surface temperature is illustrated in Figure 10 and the evolution of this variable is presented in Figure 11. The maximum temperatures are achieved at points close to the fire source, as A and D. At A_1 , the temperature is about 430°C at 1h of fire, and 425°C at A_2 at the same time. At this temperature, the steel already presents yield strength reduction. For D_1 and D_2 , the temperature is about 369°C and 363°C respectively. The temperature decreases with the distance from fire source (B, E - Figure 11) and those points are more affected by the thermal conduction (Figure 10).

This simple supported column is subjected to a vertical load of 325kN , which correspond to $1/50$ of the Euler's buckling critical load. In this way, the column will be close to a uniform stress state and remain straight; the horizontal displacements generated will be due to the thermal load applied by the fire. The von Mises stress (S) distribution is illustrated in Figure 12, together with the displacements (δ). At the beginning of the fire, the stress concentration is located at the areas close to the fire source (which also have the highest temperatures - Figure 10). The expansion of the heated flange

areas start to create a bending moment originated by the temperature gradient (Figure 12c), which will generate horizontal displacement (A, D - Figure 12d,e,h). The Young modulus and the proportional limit of stress start to decrease after the temperature achieves 100°C , at 400°C , is the yield strength that changes. Those changes in the material properties will reduce the stress state and increase the deformations at some points of the structure (Figure 11, Figure 12d,e,f,g).

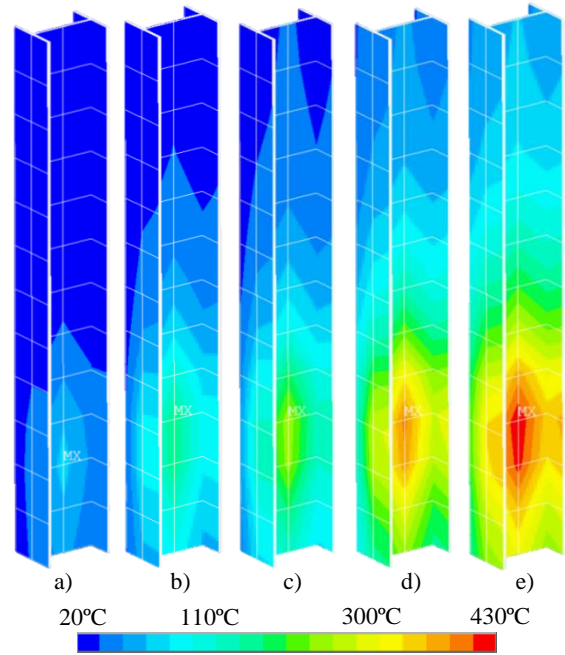


Figure 10: Distribution of the surface temperature: a) 5min; b) 10min; c) 15min; d) 30min; e) 60min.

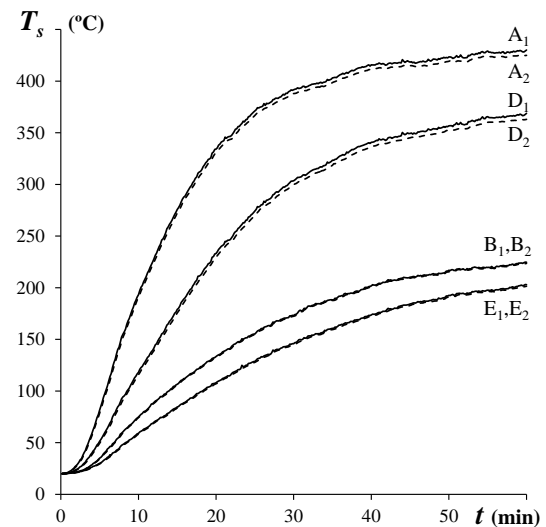


Figure 11: Evolution of the surface temperature in function of fire elapsed time.

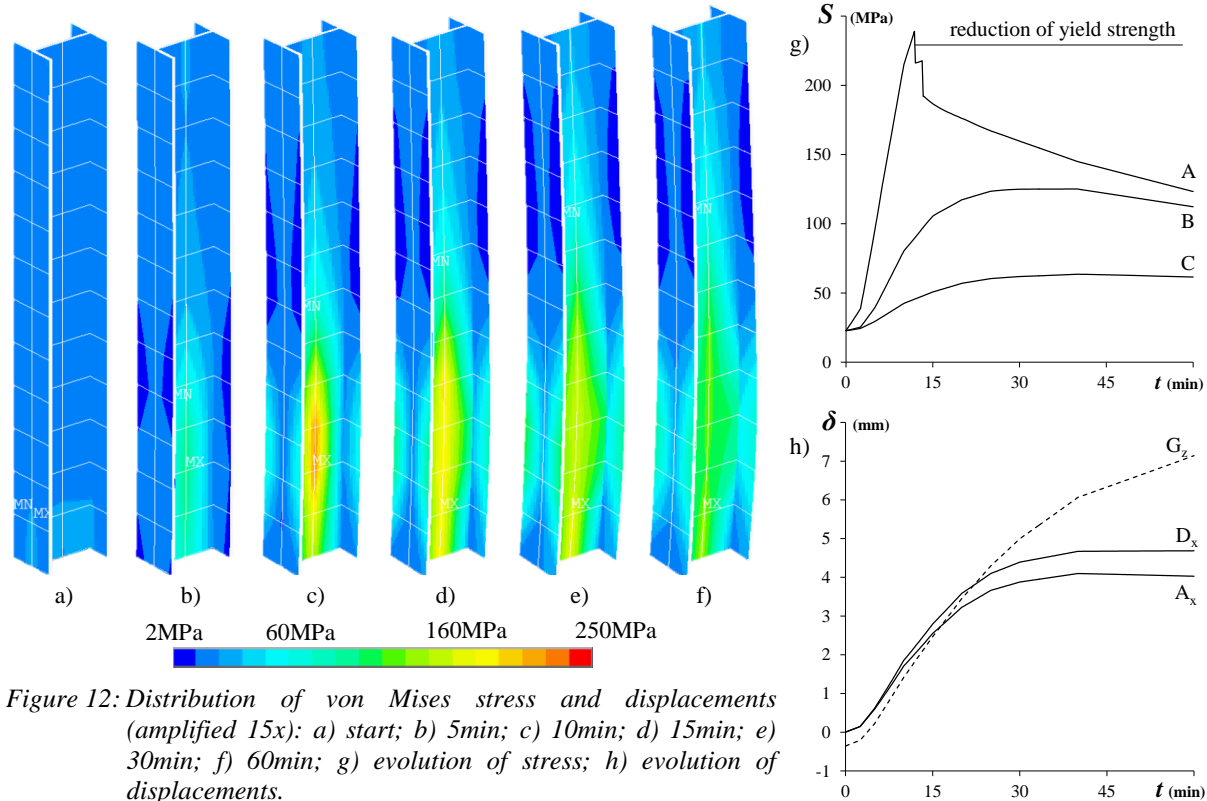


Figure 12: Distribution of von Mises stress and displacements (amplified 15x): a) start; b) 5min; c) 10min; d) 15min; e) 30min; f) 60min; g) evolution of stress; h) evolution of displacements.

As this column is simply supported, the vertical displacement is not constrained, and the thermal expansion will make this column to increase its size. The vertical displacement at the top of the column (G - Figure 8b) is presented on Figure 12h. Even with the horizontal displacements (from bending) and the vertical load, the vertical displacement at the column top is about 7mm with 1h of fire. During the analysis of global structures this expansion can lead to additional forces at other members.

Even `fds2ftmi` been ready to be applied for complex structures, as curved geometries, sloped ceilings, etc., the obtained results will be dependent of the FDS solution around the structure, e.g. radiation, heat transfer coefficient and the flow motion, which need to be handle carefully.

CONCLUSIONS

The main goal of this work is to provide a Fire-Thermomechanical Interface (FTMI) model devoted to performance-based analysis of structures under fire conditions. The application cases verified that the proposed procedure can precisely evaluate the interface between CFD and FEM models. The addition of the heat transfer coefficient distribution and the definition of the thermal exposure helped to reproduce correctly the heat flux at the FEM model.

The automated code (`fds2ftmi`) was able to extract the variables from the FDS results files and generate the boundary conditions to ANSYS, by APDL scripts, using solids and shell elements. The presented results demonstrated that this methodology can improve the reach of the fire engineering producing reliable performance-based analysis of structures under fire.

REFERENCES

- AISC/LFRD (2005), "Manual of Steel Construction - Load and resistance factor design specification for structural steel buildings", Chicago.
- Duthinh, D., McGrattan, K., Khaskiac, A. (2008), "Recent advances in fire-structure analysis", *Fire Safety Journal*, 43, 161-167.
- EN 1991-1-2 (2002), "Eurocode 1 - Actions on Structures - Part 1-2: General Actions - Actions on Structures Exposed to Fire", Comité Européen de Normalisation, Brussels.
- EN 1993-1-2 (2005), "Eurocode 3 - Design of steel structures - Part 1.2: Structural Fire Design", Comité Européen de Normalisation, Brussels.
- Kumar, S., Miles, S., Welch, S., Vassart, O., Zhao, B., Lemaire, A., Noordijk, L., Fellinger, J., Franssen, J. (2006), *Firestruc - Integrating advanced three-dimensional modelling methodologies for predicting thermo-mechanical*

behavior of steel and composite structures subjected to natural fires”, Research Programme of the Research Fund for Coal and Steel.

McGrattan, K., Hostikka, S., McDermott, R., Floyd, J., Weinschenk, C. and Overholt, K. (2013), “Fire Dynamics Simulator User's Guide, NIST Special Publication 1019 (sixth edition)”, National Institute of Standards and Technology, EUA.

Prasad, K. and Baum, H. (2005), "Coupled fire dynamics and thermal response of complex building structures", In: Proceedings of the Combustion Institute, 30, 2255–2262.

Sandström J., Wickström U. and Velkovic M. (2009), “Adiabatic Surface Temperature: A sufficient Input Data for a Thermal Model”, In: Proceedings of Application of Structural Fire Engineering”, Prague, Czech Republic, 102-107.

SAS (2009), “ANSYS Reference Manual, version 12”, Swanson Analysis Systems Inc.

Wickström U. (2004), “Heat transfer by radiation and convection in fire testing”, Fire and Materials, 28, 411-415.

Wickström, U., Duthinh, D., McGrattan, K. (2007), "Adiabatic Surface Temperature for Calculating Heat Transfer to Fire Exposed Structures", In: Proceedings of The Eleventh Interflam Conference, London, United Kingdom.

Wickström U., Robbins A. and Baker G. (2010), “The Use of Adiabatic Surface Temperature to Design Structures for Fire”, In: Proceedings of Structures in Fire (SIF), Michigan, USA, 951-958.